Bull. Inst. Chem. Res., Kyoto Univ., Vol. 53, No. 1, 1975

Monte Carlo Calculations of Energy Response for Low-Energy γ Rays in Sodium-Iodide Crystals

Takeshi MUKOYAMA*

Received December 25, 1974

A Monte Carlo method for the determination of the response function, photofraction, and total detection efficiency of sodium-iodide crystals for low-energy γ rays is described. The calculations have been carried out for point and disc sources, and for γ-ray energies less than 3 MeV. Some results obtained in the present work have been compared with experimental data and other calculated results. The influence of the source dimension on these quantities is evaluated and the effect of electron slowing down is investigated. It is shown that the response parameters for a disc source with small radius placed at a certain distance from the detector are equal to those for a point source.

I. INTRODUCTION

The wide use of scintillation counters in γ-ray spectroscopy has made it necessary to determine the characteristic energy response of sodium-iodide crystals. Although the response may be experimentally measured at certain energies using the monoenergetic γ-ray sources, the number of such nuclides are quite limited. In order to obtain the response at arbitrary energies, the theoretical calculations should be performed. The Monte Carlo method has been extensively used for this purpose. A large number of Monte Carlo calculations for sodium-iodide crystals have been carried out in various source-detector geometries.[1~11] Energy response, photofraction, and detection efficiencies of various sizes of NaI crystals have been obtained for point and disc sources, and broad and collimated parallel beams, and compared with experiments.

In practical case, the source is not point, but has a finite dimension. In the case of disc source, however, the reported results are quite limited in the source size and no systematic studies of the source-radius effect on energy response have so far been made. The aim of the present work is to provide the computer program to calculate the energy response of NaI crystals and to estimate the influence of the radius of the disc source on the energy response. Furthermore, the effect of electron slowing down is also investigated.

In the present work, the Monte Carlo method has been used to simulate the history of many photons on the digital computer. The program has been written for a point or disc source, for a circular cylindrical crystal, and for initial γ-ray energies ranging from 0.03 to 3 Mev. This program yields the energy response in the form of a histogram of the number of γ rays recorded by the NaI crystal in a given energy interval; the energy range is divided into equal intervals by the set of energy points $E(1)\sim E(100)$, where $E(100)$ is the primary energy of the γ ray, and the number of gammas recorded in the interval $[E(i-1), E(i)]$, I_i, is calculated. The photofraction and the total detection efficiency are also determined simultaneously. The photofraction is defined as the ratio

*向山 毅 : Laboratory of Nuclear Radiation, Institute for Chemical Research, Kyoto University, Kyoto.

of the number of gammas losing all the primary energy in the crystal to that interacting with the crystal, and the total detection efficiency is determined as the number of gammas interacting with the crystal, divided by the number of gammas impinging on the crystal surface.

Let N be the total number of γ rays emitted by the source into the sphere including the crystal, G be the fraction of those which strike the crystal surface, I_0 be the number of gammas which pass through the crystal without interaction, and $I=\sum_{i=1}^{100} I_i$ be the number of interacting gammas. Then the relation between N, G, I_0, and I is expressed as

$$NG=I_0+I. \tag{1}$$

The photofraction P and the total detection efficiency D are given by

$$P=\frac{I_{100}}{I}\ , \tag{2}$$

$$D=\frac{I}{NG}\ . \tag{3}$$

Using these expressions, the photopeak efficiency frequently used for determination of the source intensity is written by

$$PE=\frac{I_{100}}{N}=P\cdot D\cdot G. \tag{4}$$

The geometrical efficiency G can be calculated analytically for the source-to-detector geometry considered here.

II. METHOD OF CALCULATION

The computer programs have been written for the following three cases;

Case I: A disc source the center of which is on the crystal axis. The secondary electrons produced in the crystal are assumed to be completely absorbed.

Case II: A point source on the crystal axis. The secondary electrons are assumed to be completely absorbed.

Case III: A point source on the crystal axis. The secondary electrons are traced.

In all cases, Rayleigh scattering and bremsstrahlung radiation are not taken into account.

The flow diagram in Fig. 1 shows for Case III how each photon history is followed until the photon either is absorbed or escapes from the crystal. In Cases I and II, the flow diagrams are quite similar to Fig. 1, except that the electron tracing routines in photoelectric effect, Compton scattering, and pair production are omitted.

All the calculations in the present work have been carried out on the KDC-II computer[12] in the Computer Center of Kyoto University.

A. Random Numbers

All the random numbers used in the present calculations are generated by the computer as to distribute uniformly in the interval [0, 1]. The congruence method

$$r_i=r_{i-1}*5^{11}\ (\mathrm{Mod}\ 2^{31}), \tag{5}$$

is used for this purpose.

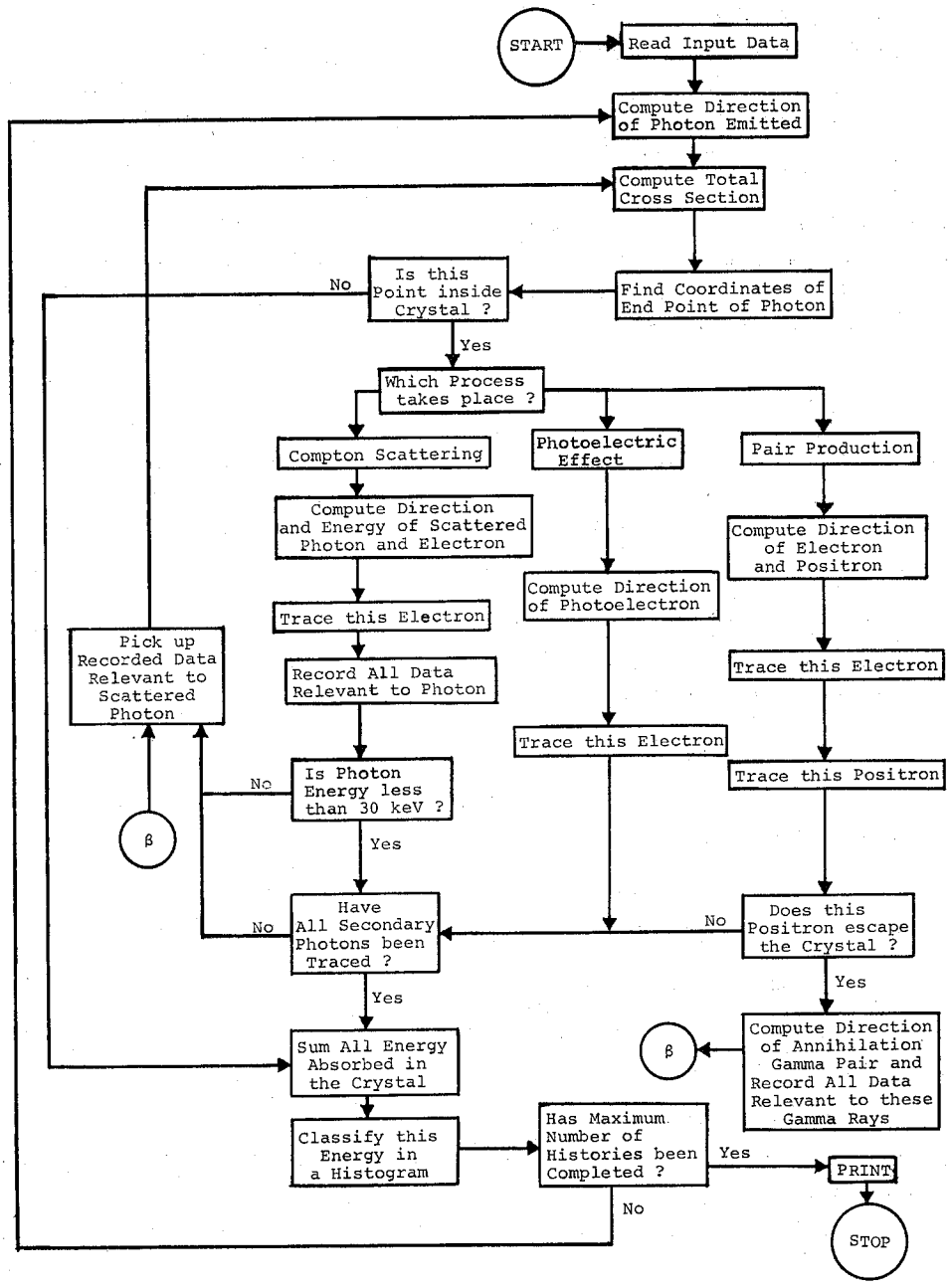

Fig. 1. Schematic flow diagram for Case III.

B. Cross Sections

The gamma-ray cross sections in NaI for Compton scattering, photoelectric effect, and pair production are taken from the tabulation of Grodstein.[13] Table of these cross sections for energy region concerned is stored in the program and the values at intermediate energies are obtained by interpolation.

C. Sampling the Source

Two different sampling techniques are used in the present work.

(1) For a disc source in Case I, a point on the disc source is randomly selected, and the direction of emission of gamma is isotropically chosen. Then the position on the crystal which the photon impacts is determined. If the photon does not strike the crystal surface, this procedure is repeated again.

(2) For a point source in Cases II and III, direction of photon emission is selected by the systematic sampling technique.[14] When z axis is taken along the detector axis and the origin is at the face of the detector nearest the source, the direction cosine of the i-th history of photons emitted from the source with respect to z axis is given by

$$\gamma=(1-\gamma_0)(i-r_i)/N+\gamma_0, \quad i=1, 2, \ldots, N, \tag{6}$$

where r_i is the random number, N is the total number of histories, and γ_0 is the minimum cosine with respect to the z axis subtended by the detector. In this case, the other direction cosines are $\alpha=(1-\gamma^2)^{1/2}$ and $\beta=0$, and the position at which the photon impacts the crystal surface is given by $x=\alpha d/\gamma$, $y=0$, and $z=0$, where d is the source-to-detector distance.

D. Distance Travelled by the Photon

The position of the interaction within the crystal is determined by random sampling of the exponential distribution:

$$R=-1/\tau_{\text{total}} \ln r, \tag{7}$$

where r is a uniform random number on the interval [0, 1] and τ_{total} is the total γ-ray attenuation coefficient in NaI.

E. Classification of Interactions

The choice of the type of interaction is taken to be given by the relative probability

$$\tau_{\text{compton}}/\tau_{\text{total}},\ \tau_{\text{photo}}/\tau_{\text{total}},\ \tau_{\text{pair}}/\tau_{\text{total}}.$$

Once the type of interaction is determined, the program is made to be branched to this particular interaction path.

F. Photoelectric Effect

In photoelectric effect, the photon is absorbed by an atom and the photoelectron appears with the energy

$$E_e=E-B_K, \tag{8}$$

where E is the energy of incident γ ray and B_K is the binding energy of K electrons in iodine. For unpolarized γ rays, the differential cross section for photoelectric effect is given by Sauter.[15] Sugiyama[16] devised the selection technique for obtaining the polar angle of the photoelectron from the Sauter's formula. He used the method proposed by Butcher and Messel,[17] which is in combination of the rejection method with the composition method. In Fig. 2 is shown the flow diagram of this method. In the figure, $A=1+E_e/2mc^2$, β is the ratio of the velocity of the electron to that of light in vacuum, $\varepsilon=1/(1-\beta)$, $\delta=1/(1+\beta)$, $S_0=(\varepsilon^3-\delta^3)/3$, $S_1=\delta^2(\varepsilon-\delta)$, $S_0'=(\varepsilon^2-\delta^2)/2$, and $S_1'=\delta(\varepsilon-\delta)$.

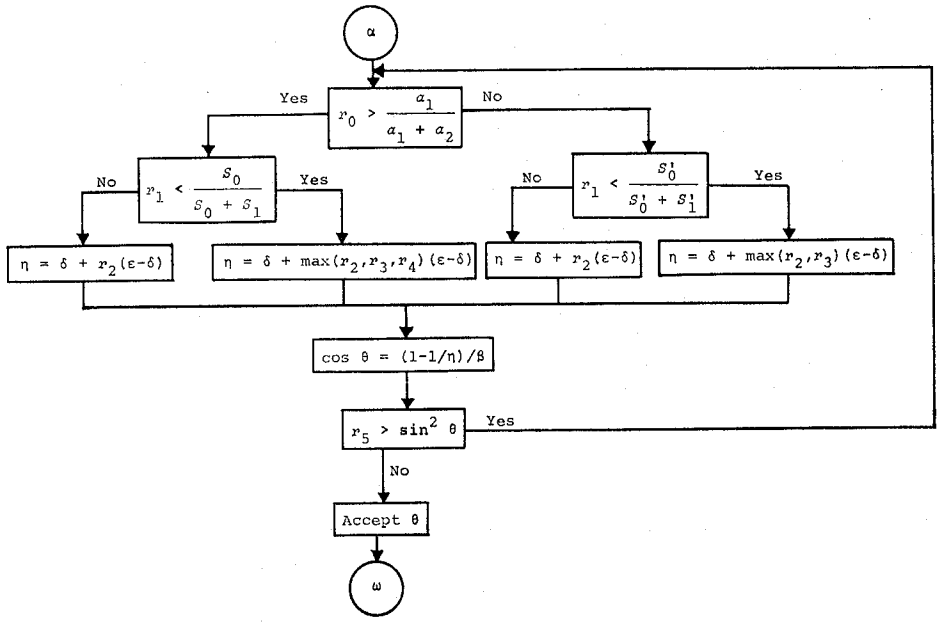

Fig. 2. Method of randomly selecting the cosine of the polar angle of the photoelectron.

The fluorescent K x-ray is emitted in filling the K hole produced as a consequence of the photoelectric effect. The K fluorescence yield for NaI is about 83%. The x rays are emitted isotropically with energy of about 33 keV. Since this energy is small, x rays produced by the photoelectric effect are considered to be completely absorbed in the crystal.

G. Compton Scattering

In Compton scattering, the energy and momentum of the incident photon are changed and the energies for the scattered photon and the recoil electron for each scattering angle are determined by the conservation law. For unpolarized radiation, the polar angle of the scattering of the photon is determined by random sampling of the famous Klein-Nishina formula.

Figure 3 represents the flow diagram of Kahn's rejection method which selects the cosine of the polar angle of scattering, μ, and the wave length of the photon after scattering, λ_{n+1}.[18]

The polar angle of the recoil electron is obtained from the polar angle of the scattered photon, θ, using the law of momentum conservation:[19]

$$\cot \theta' = (1+\alpha) \tan \frac{\theta}{2} , \qquad (9)$$

where α is the energy of the incident gamma in unit of rest mass of the electron.

The azimuthal angles of the scattered photon and recoil electron are sampled from the uniform distribution in the interval $[0, 2\pi]$ by the use of the von Neumann's technique described later.

H. Pair Production

In pair production, the incident photon disappears and an electron-positron pair is

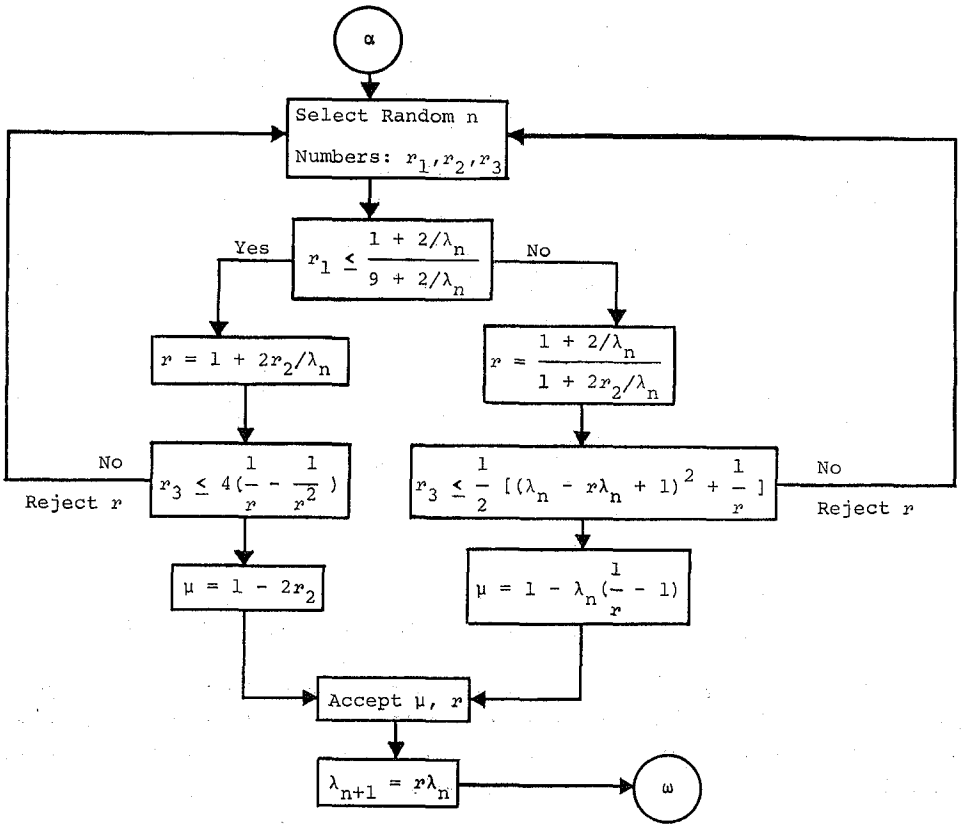

Fig. 3. Kahn's method of randomly selecting the cosine of the polar angle and the energy of the scattered photon in Compton effect.

created. It is assumed that the kinetic energy exceeding the pair-production threshold is shared equally by the electron and positron:

$$E^+ = E^- = \frac{1}{2}(E - 2mc^2). \tag{10}$$

Under this approximation, the polar angle of the pair-produced electron and positron with respect to the direction of the incident photon is given by[20]

$$\theta^{\pm} \simeq mc^2/E^{\pm}. \tag{11}$$

Such an estimation is only approximate, but it can be considered as the average value of a great many number of the events. The azimuthal angles for the electron and positron are uniformly distributed, but differ by 180°.

I. Annihilation Radiation

The positron created in the pair-production effect is followed as the electron. The annihilation of the positron is assumed to take place at rest, and if the position where the range of the positron terminates is in the crystal, two photons are generated at the end of the positron path, each having an energy of 511 keV. The first photon is emitted in a random direction and the second a direction opposite to the first.

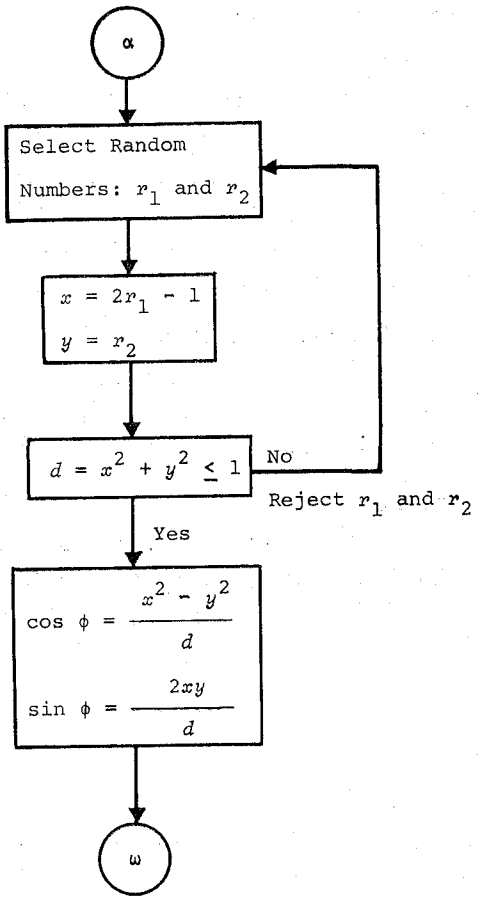

Fig. 4. Von Neumann's method of randomly selecting the uniformly distributed azimuthal angle.

J. Slowing Down of Electrons and Positrons

The path of the electron and positron produced by Compton scattering, photoelectric effect, and pair production is assumed to be straight. The slowing down of these electrons is treated by the Wilson's theory which includes excitation and ionization losses and radiation loss in the field of the nucleus.[21] The mean distance travelled by an electron (or positron) with the initial kinetic energy E, measured in radiation length, is given by

$$R=\ln 2\cdot\ln\left(\frac{E}{E_c \ln 2}+1\right), \tag{12}$$

where E_c is the so-called critical energy in the same unit as E.

If the end of the path determined from the mean range R is outside the crystal, the energy carried away by the escaping electron is obtained by the use of the distance travelled outside the crystal, R', from

$$E'=[\exp(R'/\ln 2)-1]E_c\cdot\ln 2, \tag{13}$$

and the energy absorbed by the crystal is given by $E-E'$. The values of the critical

energy and radiation length are evaluated for NaI as 17.6 MeV and 2.47 cm, respectively.[20]

K. Selection of a Uniformly Distributed Azimuthal Angle

The selection of a random azimuthal angle, ϕ, from a uniform distribution on the interval $[0, 2\pi]$ is replaced by the selection of the sine and cosine of the azimuthal angle, because in usual case the trigonometric functions of ϕ are required instead of the angle itself. Figure 4 shows the von Neumann's method of randomly selecting $\sin\phi$ and $\cos\phi$ where ϕ is uniformly distributed on the interval $[0, 2\pi]$.[22]

L. Selection of a Random Isotropic Direction

The selection of a random isotropic direction is made by randomly selecting the direction cosines of an isotropic vector. In Fig. 5 the flow diagram of the Coveyou's method is shown.[14] The constant A in the figure is taken to be $3^{1/2}/4^{2/3}$.

M. Rotation of Coordinates

If the cosine of the polar angle of scattering is μ, the azimuthal anlge is ϕ, and the direction cosines of the initial direction are α, β, and γ, the direction cosines of the scattered photon and electron, α', β', and γ', are determined from the flow diagram in Fig. 6.[14]

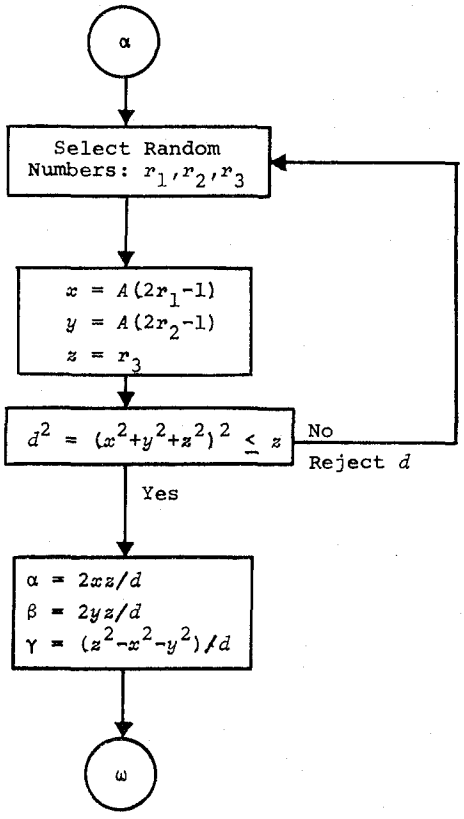

Fig. 5. Coveyou's method of randomly selecting the direction cosines of an isotropic vector.

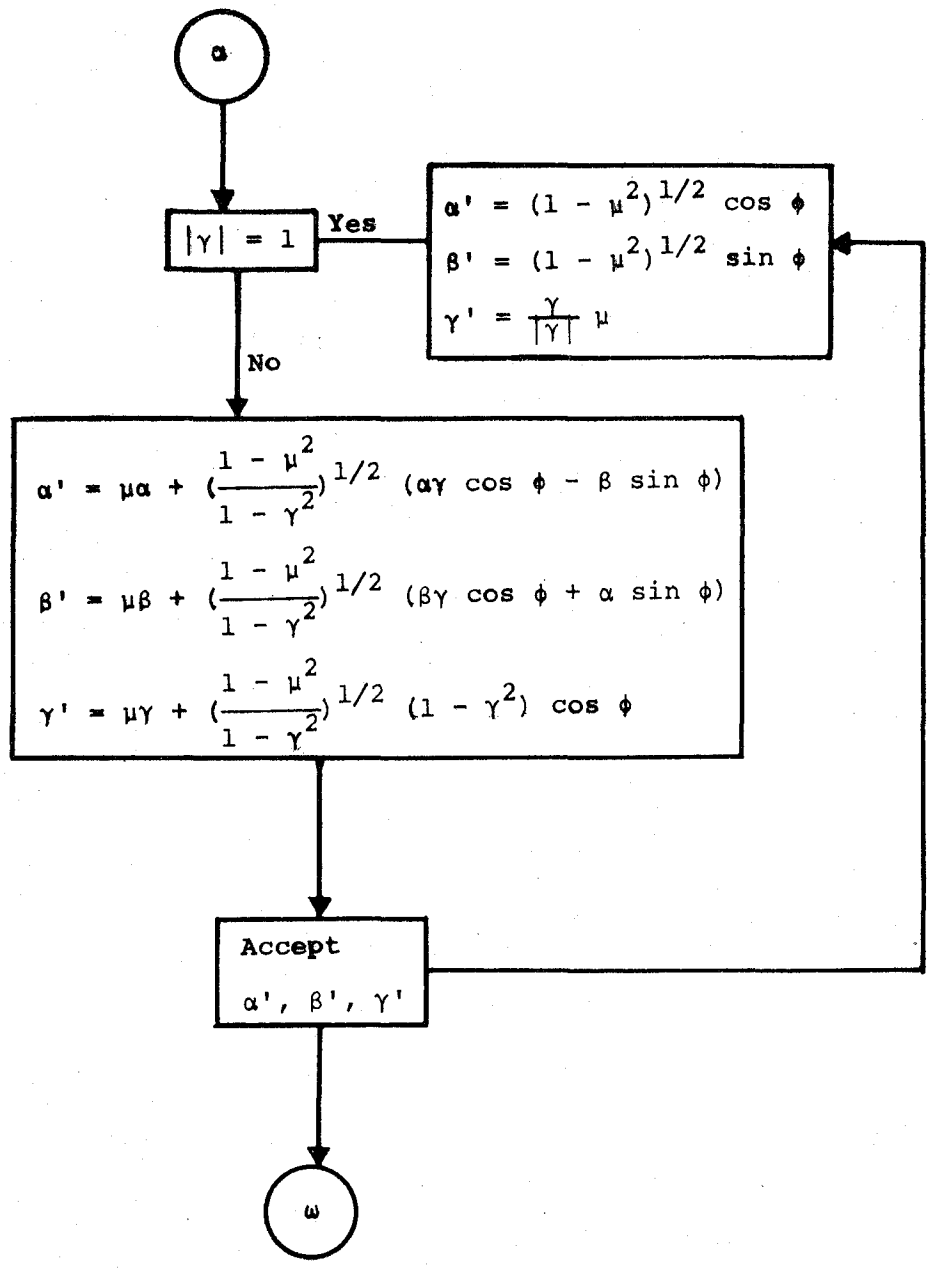

Fig. 6. Rotation of coordinates to obtain the direction cosines after the scattering.

III. RESULTS AND DISCUSSION

To test the present calculations, comparisons were made with the other calculated and experimental results. Table I shows a comparison of total detection efficiencies and photofractions for an isotropic point source placed at 10 cm from the surface of a 3″×3″ NaI crystal. The calculations were made for 10000 histories using the program for

Table I. Comparison of the Present Results (Case III) with Calculated and Experimental Data for a 3″×3″ NaI Crystal. An Isotropic Point Source is Placed at 10 cm from the Crystal.

E_0 (MeV)	Total detection efficiency			Photofraction								
	Calculated			Calculated						Experimental		
	Present work	Ref. 4	Ref. 11	Present work	Ref. 4	Ref. 5[a]	Ref. 8[b]	Ref. 9	Ref. 11	Ref. 23	Ref. 24	Ref. 25
0.145	0.936	0.936		0.973	0.959							
0.279	0.816	0.811		0.884	0.861							
0.323	0.772		0.76	0.826	0.815[a]	0.832	0.84	0.835	0.85	0.820	0.77	0.83
0.662	0.623	0.619	0.60	0.550	0.562	0.569	0.56	0.551	0.57	0.536	0.51	0.58
1.17	0.528	0.525	0.52	0.395	0.410	0.384	0.39	0.398	0.42	0.383	0.34	0.40
1.33	0.509	0.509	0.49	0.365	0.392	0.326	0.37	0.372	0.39	0.357[a]	0.31	0.35
2.75	0.436		0.43	0.232	0.254[a]	0.196	0.21	0.229	0.24	0.225	0.18	0.21

[a] Data taken from Ref. 9. [b] Data taken from Ref. 11.

Case III. It can be said from the table that the predicted values are in fairly good agreement with the values of other workers.

In Table II the results obtained in Case I for a disc source located on the crystal axis at a distance of 10 cm from a 3″×3″ NaI crystal are compared with other theoretical calculations. The radius of the source is taken to be equal to that of the crystal. The values for total detection efficiency are in good agreement with those of Miller and Snow.[4] However, the present values for photofraction are larger than their values. This is because in the program for Case I no account is taken of the energy loss and leakage of the secondary electrons produced in the crystal.

In order to estimate the effect of electron slowing down on the response parameters, the calculations were performed using three programs for a point source placed at 10 cm from a 3″×3″ crystal. In Case I, the results were evaluated by taking the radius of the disc source to be zero. The calculated values are compared in Table III. The difference between Cases I and II is the source sampling technique. It appears that the systematic sampling technique (Case II) gives slightly smaller photofractions for high-energy photons

Table II. Comparison of the Present Results (Case I) with Other Calculations for a 3″×3″ NaI Crystal. An Isotropic Disc Source with Radius Equal to the Crystal Radius is Placed at 10 cm from the Crystal Surface on the Crystal Axis.

E_0 (MeV)	Total detection efficiency		Photofraction		
	Present work	Ref. 4	Present work	Ref. 4	Ref. 10[a]
0.145	0.946	0.936	0.980	0.959	
0.662	0.641	0.619	0.613	0.562	0.547
1.17	0.555	0.525	0.466	0.410	
1.33	0.530	0.509	0.431	0.389	0.409
2.62	0.452	0.428	0.309	0.260	0.252
2.75	0.454		0.303		

[a]Source thickness is 0.001 cm.

Table III. Comparison of the Present Results in Three Cases for a 3″×3″ NaI Crystal. An Isotropic Point Source is Placed at 10 cm from the Crystal on the Crystal Axis.

E_0 (MeV)	Total detection efficiency			Photofraction		
	Case I	Case II	Case III	Case I	Case II	Case III
0.145	0.938	0.937	0.936	0.979	0.979	0.973
0.662	0.620	0.629	0.623	0.608	0.604	0.550
1.17	0.530	0.531	0.528	0.465	0.444	0.395
2.75	0.427	0.430	0.436	0.304	0.282	0.232

than the analogue procedure (Case I). However, in the low-energy region both methods agree very well. Comparison of the photofractions for Case II with those for Case III indicates that the energy loss and leakage of the secondary electrons are important in

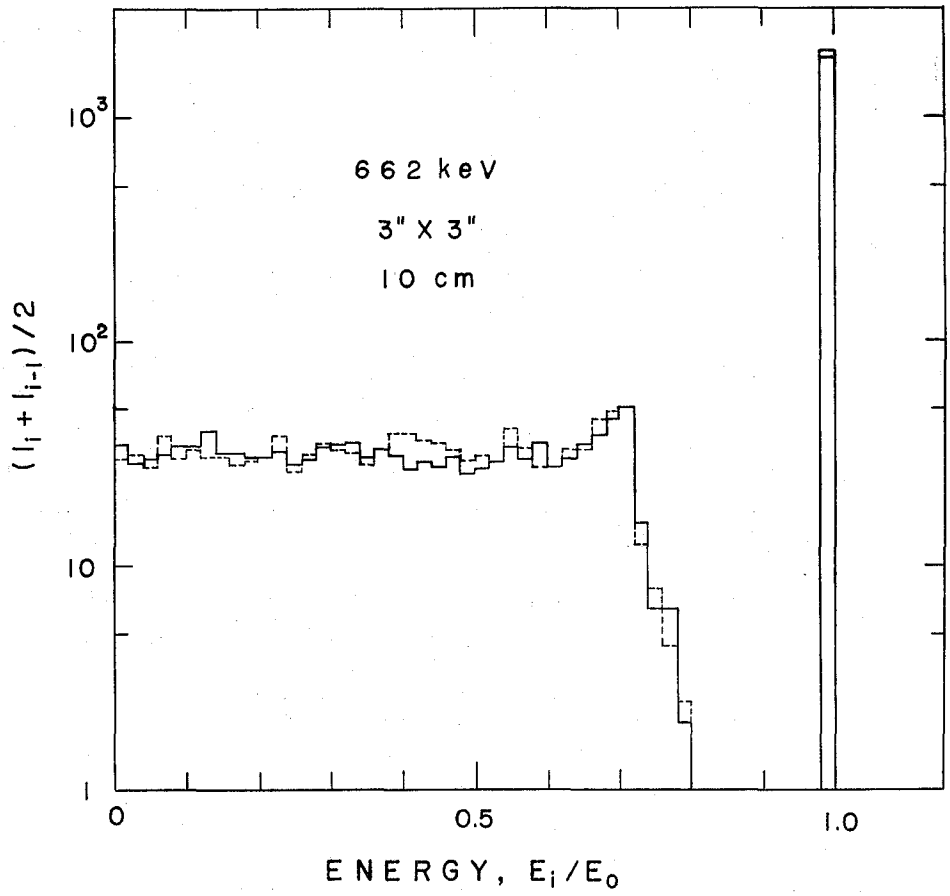

Fig. 7. Calculated response functions for a 3″×3″ NaI crystal. The full line represents a point source placed at 10 cm from the crystal and the dashed line represents a disc source with radius equal to the crystal radius, located at 10 cm from the crystal. The γ-ray energy is 662 keV.

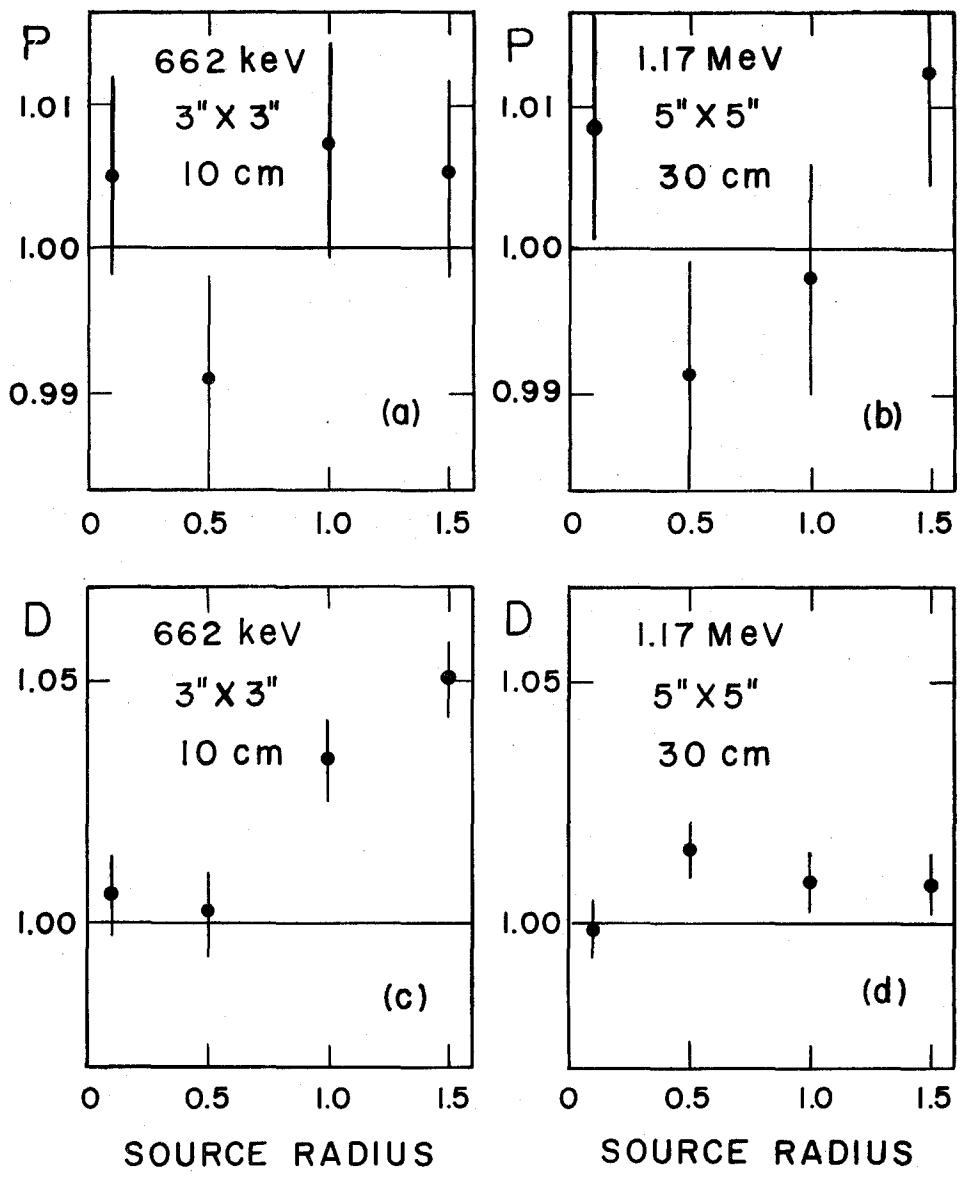

Fig. 8. Calculated relative photofraction and relative total detection efficiency as a function of the source radius. (a) and (c); a 662-keV source is placed at 10 cm from a 3″×3″ NaI crystal. (b) and (d); a 1.17-MeV source is placed at 30 cm from a 5″×5″ NaI crystal. Photo fraction and total detection efficiency are expressed as a ratio to the value for a point source, and source radius is expressed as a ratio to the crystal radius.

estimation of the response parameters, except for low-energy gamma rays.

To investigate the response parameters of the crystal as a function of the source radius, the program for Case I has been used. The crystal sizes were chosen to be 1″×1″, 3″×3″, and 5″×5″. In all cases the disc sources having radius equal to 0.1, 0.5, 1.0, and 1.5 times as large as the crystal radius were placed on the crystal axis and the distances

between the source and crystal were taken to be 10 and 30 cm. The total number of histories of photon impinging on the crystal surface is 10000. In the following, only typical examples which give the general trend are shown in the figures.

Figure 7 shows the calculated response functions for a $3'' \times 3''$ crystal for a point source and a disc source with radius equal to the crystal radius. In both cases the 662-keV sources are placed at a distance of 10 cm from the crystal surface. It can be seen from the figure that the source-radius effect causes no appreciable change in the response function. This fact is confirmed for all other source-crystal arrangements described above.

In Fig. 8 the relative photofractions and relative total detection efficiencies versus the source radius are shown. These response parameters are expressed as a ratio to the value for a point source and the source radius are given in the ratio to the crystal radius. The error bars in the figure indicate the standard deviation. It is shown that the change in photofractions due to the source radius is small. In all cases considered here it can be said that the photofractions are equal within the statistical fluctuation.

On the other hand, the total detection efficiency slightly increases for small source-to-detector distance, for large source radius, and for high γ-ray energy. When the source-to-detector distance is 30 cm, the effect of the source radius gives a maximum increase of 1.5%. In the case of the distance of 10 cm, the total detection efficiency of the source whose radius is equal to the crystal radius increases by about 5% for a $3'' \times 3''$ and by about 10% for a $5'' \times 5''$ crystal, for photon energies higher than 662 keV. This increase can be attributed to the largeness of the mean angle of incidence of the photons. If the source-to-dectetor distance is small and the source radius is large, the number of high-energy photons passing through the crystal without any interaction decreases because the mean path length of the gammas impinging on the crystal obliquely becomes large.

In conclusion, when the source radius is smaller than a half of the crystal radius and the source-to-detector distance is larger than 10 cm, the influence of the source radius on the response parameters is negligibly small. It should be noted, however, that the photopeak efficiency defined in Eq. (4) depends on the source radius, because the geometrical efficiency G decreases with the source radius.

ACKNOWLEDGMENT

The author wishes to express his thanks to Professor S. Shimizu for his encouragement throughout the present work.

REFERENCES

(1) W. F. Miller, J. Reynolds, and W. J. Snow, ANL-5902 (Argonne National Laboratory, 1958).
(2) C. M. Davisson and L. A. Beach, NRL-5408 (S. U. Naval Research Laboratory, 1959).
(3) W. F. Miller and W. J. Snow, *Rev. Sci. Instr.*, **31**, 39 (1960).
(4) W. F. Miller and W. J. Snow, ANL-6318 (Argonne National Laboratory, 1961); *Nucleonics*, **19**, No. 11, 174 (1961).
(5) C. D. Zerby and H. S. Moran, *Nucl. Instr. and Meth.*, **14**, 115 (1961).
(6) C. Weitkamp, *Nucl. Instr. and Meth.*, **23**, 13 (1963).
(7) B. J. Snyder and G. F. Knoll, *Nucl. Instr. and Meth.*, **40**, 261 (1966).
(8) B. J. Snyder, *Nucl. Instr. and Meth.*, **46**, 173 (1967).
(9) M. Giannini, P. Oliva, and M. C. Ramorino, *Nucl. Instr. and Meth.*, **81**, 104 (1970).

(10) T. Nakamura, *Nucl. Instr. and Meth.*, **105**, 77 (1972).
(11) M. Belluscio, R. De Leo, A. Pantaleo, and A. Vox, *Nucl. Instr. and Meth.*, **118**, 553 (1974).
(12) Kyoto University Digital Computer No. 2; Commercial Name is HITAC 5020.
(13) G. White Grodstein, NBS Circular 583 (1957).
(14) C. D. Zerby, "Methods in Computational Physics," Vol. 1, ed. by B. Alder, S. Fernbach, and M. Rotenberg, Academic Press, New York, 1963, p. 90.
(15) F. Sauter, *Ann. Physik*, **11**, 454 (1931).
(16) H. Sugiyama, Researches of the Electrotechnical Laboratory, Japan, No. 724 (1972).
(17) J. C. Butcher and H. Messel, *Phys. Rev.*, **112**, 2096 (1958).
(18) H. Kahn, *USAEC Report No. AECU-***3259** (1954).
(19) R. D. Evans, "Handbuch der Physik," Vol. 34, ed. by S. Flügge, Springer, Berlin, 1958, p. 218.
(20) H. A. Bethe and J. Ashkin, "Experimental Nuclear Physics," Vol. 1, ed. by E. Segre, Wiley, New York, 1953, p. 166.
(21) R. R. Wilson, *Phys. Rev.*, **79**, 204 (1950); **84**, 100 (1951).
(22) J. von Neumann, "Monte Carlo Method," Natl. Bur. Standards Appl. Math. Ser. No. 12, p. 36 (1951).
(23) R. L. Heath, *USAEC Report No. IDO-***16680** (1964); R. L. Heath, R. G. Helmer, L. A. Schmittroth, and G. A. Cazier, *USAEC Report No. IDO-***17017** (1965).
(24) H. Leutz, G. Schultz, and L. van Gelderen, *Nucl. Instr. and Meth.*, **40**, 257 (1966).
(25) B. Chinaglia and R. Malvano, *Nucl. Instr. and Meth.*, **45**, 125 (1966).